

Biomechanical Effects of the Geometry of Ball-and-Socket Intervertebral Prosthesis on Lumbar Spine Using Finite Element Method

Jisu Choi¹, Dong Ah Shin² and Sohee Kim¹

¹Department of medical system engineering, Gwangju Institute of Science and Technology, Cheomdan-gwagi-ro, Gwangju, South Korea

²Department of Neurosurgery, Yonsei University College of Medicine, Seoul, South Korea

Keywords: Lumbar Artificial Disc, Total Disc Replacement, Finite Element Method (FEM).

Abstract: The purpose of this study was to analyze the biomechanical effects of three different types of ball-and-socket geometry of a lumbar artificial disc using finite element method. A three dimensional linear finite element (FE) model was developed, and the lumbar artificial disc was inserted at L3-L4 level. The height of implant was fixed and location of implant was also center-fixed. Three different curvatures of ball-and-socket geometry were modeled (radius of curvature: 50.5mm for C1, 26mm for C2, 18.17mm for C3). The biomechanical effects including range of motion (ROM), stress of intervertebral disc, facet contact force and stress on implant were compared among different geometries. As the radius of curvature decreased, the result shows that ROM increased at the surgical level and the stress on implant decreased. The change in stress within intervertebral disc was not significant. The facet contact force at surgical level was maximum with C2 while C1 and C3 had similar facet contact force. We confirmed that the geometry of artificial disc can cause remarkable biomechanical changes at surgical level.

1 INTRODUCTION

Total disc replacement (TDR) has been accepted as a better treatment due to its various advantages over spinal fusion methods in degenerative disc disease (Mayer and Korge, 2002). TDR preserves disc height and inter-segmental range of motion. In addition, adjacent level effect is lower than conventional fusion methods (Panjabi et al., 2007). Although TDR has many advantages, complications have been reported (Bertagnoli et al., 2006). The system can cause facet arthrosis and excessive motion at surgical level, and it also has potential to generate subsidence of metallic endplate of the implant. In order to understand the reasons for complications, many of previous studies have used finite element analysis (Rohlmann et al., 2005), (Rundell et al., 2008). The surgical methods such as preserving the annulus fibrosus, positioning the implant, and re-suturing the anterior longitudinal ligament could affect the motion biomechanically. In addition, the size of facet joint gap leads different biomechanical changes such as facet contact force at

surgical level. Although various factors were investigated, the effect of implant geometry has not been analysed. In the present study, the artificial disc is based on ball-and-socket type, but the curvature of ball-and-socket can vary. Accordingly, we aim to investigate the effect of the curvature of ball-and-socket implant and compare the biomechanical effects at the adjacent and surgical levels of lumbar spine using finite element method (FEM).

2 METHODS

A three dimensional linear finite element model was developed and validated based on the study by Yamamoto et al. The surgical finite element model was constructed based on this validated model. The height and location of implant were fixed and only the curvature of ball-and-socket geometry was varied. Three surgical FE models with different implant geometries were constructed and compared.

2.1 Finite Element Model

The computed tomographic scan data of a healthy 24-year-old male was taken and reconstructed to three dimensional geometry using Mimics software (Materialise Inc., Leuven, Belgium). The 3D geometry was imported to Hypermesh software (Altair Engineering, Inc., Troy, MI, USA) and converted from surface to solid type. Then, it was meshed with finite elements. The cortical bone was obtained from cancellous bone's surface and cartilage endplate was extracted from the surface of intervertebral disc. The final FE model has five vertebrae (L1-L5), four intervertebral discs, and ligaments. The total number of nodes and elements were 398,260 and 945,960, respectively.

2.2 Material Properties

The material properties of each component were obtained from previous literatures (Table1). Nucleus pulposus has nearly incompressible property. Annulus fibrous ground was modeled to be linear elastic, and annulus fibers were not modeled in this study. Ligaments were modeled to be linear elastic, in which only tension can occur.

Table 1: Material properties of the used FE model.

Components	Young's Modulus (MPa)	Poisson's ration	Reference
Cortical bone	5000	0.3	Rohlmann et al. 2006b
Cancellous bone	50	0.2	Rohlmann et al. 2006a
Posterior bone	3500	0.25	Rohlmann et al. 2005
Nucleus Pulposus	1	0.499	Chen et al Goel et al
Annulus fibrous	2	0.45	Lavaste et al. 1992
Cartilage endplate	24	0.4	Goel et al.1995a
Ligaments			
ALL	20		
PLL	20		
CL	32.9		
ITL	58.7	0.45	Goel et al. 1995a
ISL	11.6		
SSL	15		
Metallic endplate	210000	0.3	Liau JJ
Polyethylene inlay (UHMWPE)	1016	0.46	Liau JJ

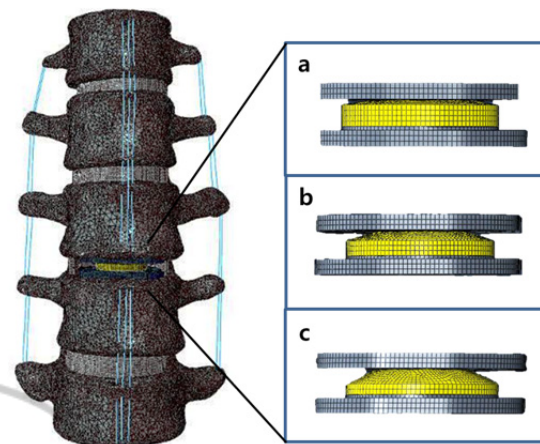


Figure 1: The surgical FE model with artificial disc at L3/4 level and different curvatures of ball-and-socket geometry. (C1: 50.5mm, C2: 26mm, C3: 18.17mm).

The FE model was exported to Abaqus software (ABAQUS 6.13.; Hibbit, Karlsson&Sorenson, Inc., Providence, RI, USA) after the material properties were applied to each component of lumbar spine in the model.

2.3 Surgical FE Model

The artificial disc was modeled to be 34.5mm, 27mm, and 2mm in width, length, and thickness, respectively. The implant height was designed to be 8.7mm to fit the FE model. The implant was modeled to have three different radii of curvature (50.5mm for C1, 26mm for C2, 18.17mm for C3) and inserted at L3-L4 level. Following the standard surgical method, anterior longitudinal ligament and Nucleus pulposus were removed and only lateral Annulus fibrous was remained. The implant was located at the center of vertebral body. The coefficient of sliding contact between ball-and-socket was 0.07 (Godest et al., 2002). The tie interaction was applied to the endplates of implant and vertebrae for complete fusion. The surgical FE model is shown in Figure 1.

2.4 Boundary and Loading Condition

For validation of the intact FE model, we followed the same protocol used in the study of Yamamoto et al. The moment of 10 Nm was applied to the superior surface of L1, and the inferior surface of L5 was fixed in all directions. The same boundary and loading conditions were also applied to the surgical models.

3 RESULTS

3.1 Model Validation

To validate the FE model, the range of motion of FE model was compared with the results of the study by Yamamoto et al (Yamamoto et al., 1989). The results were within ± 1 standard deviation of the average of Yamamoto et al's study in all motion (Figure 2).

3.2 Range of Motion

There was no significant difference among all groups at the adjacent level (L2/3, L4/5). However, at surgical level, the ROM in C1, C2 and C3 models was changed by +38.5%, +46.2%, and +57.7% in extension, -33.3%, -22.2%, and -12.7% in flexion, -5%, +30%, and +35% in bending, +191%, +4.3%, and +30.4% in torsion, respectively compared to the intact model. The results are shown in Figure 3.

3.3 The Stress of Intervertebral Disc

The stress of intervertebral disc at adjacent level (L2/3, L4/5) was within +2.4% of that of the intact model (Figure 4).

3.4 The Facet Contact Force

The facet contact force at the adjacent level (L4/5) was not significantly changed. At the surgical level, the facet contact force in C1, C2 and C3 models was changed by -4.2%, +5.9%, and -19% in extension, +81.9%, +172.3%, and +76.9% in lateral bending, +116.2%, +140.5%, and +107.9% in axial torsion, respectively compared to the intact model. The facet contact force was maximum in C2, and minimum in C3 (Figure 5).

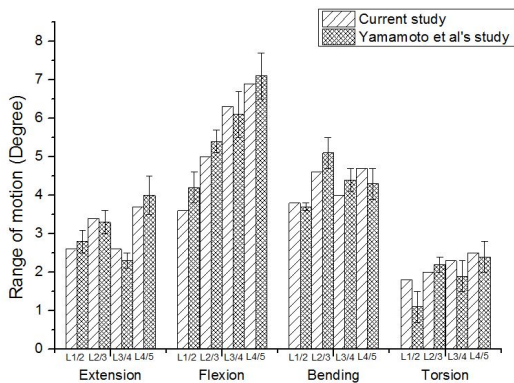


Figure 2: Comparison of range of motion between current study and Yamamoto et al's study.

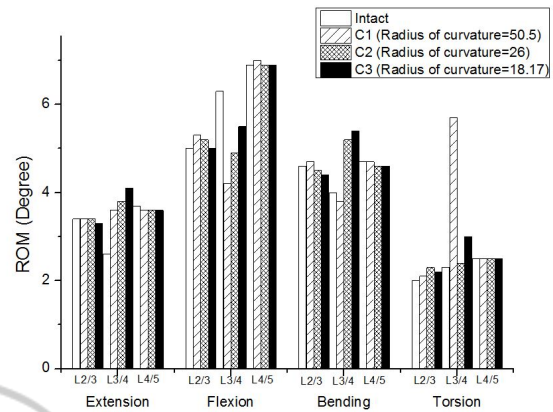


Figure 3: The range of motion with the different curvatures of implant in extension, flexion, bending and torsion at adjacent and surgical level.

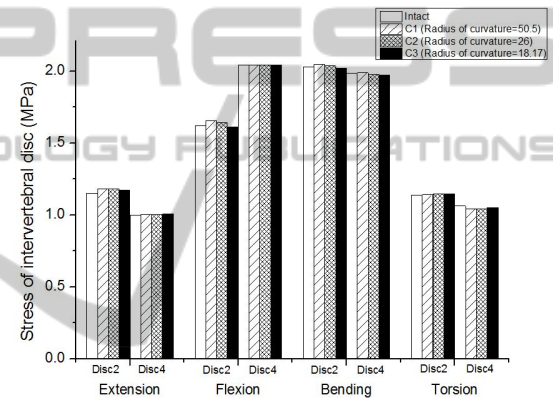


Figure 4: The stress of intervertebral disc with the different curvatures of implant in extension, flexion, bending and torsion at adjacent level.

3.5 The Stress on Implant

The stress on implant decreased with the higher degree of curvature in extension, flexion, and lateral bending. In axial torsion, intact and surgical models had relatively similar level of the stress on implant (Figure 6).

4 DISCUSSION

In this study, we investigated the biomechanical changes according to different curvatures of ball-and-socket implant. Other factors that may affect the result, such as the surgical method, location and height of implant were fixed and only the curvature of ball- and-socket was varied.

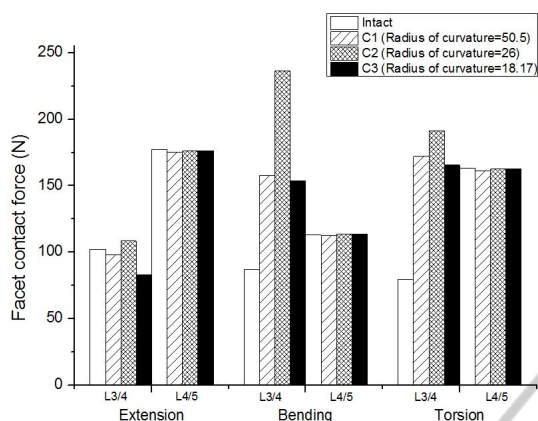


Figure 5: The facet contact force with the different curvatures of implant in extension, bending and torsion at L3/4 and L4/5 level.

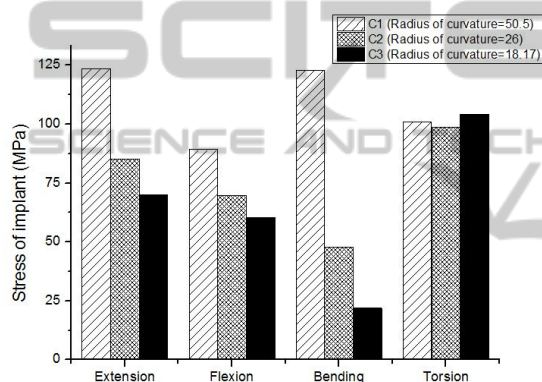


Figure 6: The stress on implant with the different curvatures of implant in extension, flexion, bending and torsion.

The range of motion, stress of intervertebral disc, facet contact force, and stress on implant were investigated with different curvatures.

The results show that the geometry of ball-and-socket artificial disc caused remarkable biomechanical changes at surgical level.

The general effects after inserting artificial disc such as increase in ROM and facet contact force at surgical level were similar to previous FE model study (Chen et al., 2009). In this study, the range of motion increased in extension, bending, and torsion after TDR. However, the ROM decreased in flexion after TDR. The reason for decreasing ROM in flexion can be attributed to the location of implant. A previous study related to TDR and intersegmental rotation reported that even slightly anterior position can cause significant ROM decrease in flexion (Rundell et al., 2008). Accordingly, the location of implant in this study could be slightly anterior rather than center location. This issue, however, was not

critical because we focused on the geometry of implant with fixed location. Also, the results were in agreement with the previous study except for flexion. In addition, the facet contact force increased after inserting artificial disc as was reported by previous studies (Kim et al., 2010).

The biomechanical effects according to the geometry of implant at surgical level, such as the ROM, facet contact force were significantly affected. In addition, the stress on implant was also affected by geometry of implant.

The entire ROM increased with decreasing radius of curvature in extension, flexion, and lateral bending. In axial torsion, ROM was maximum with the largest radius of curvature. It was speculated that the smaller radius of curvature enables the wider range of motion, but the central point of rotation axis misplaces in axial rotation.

The geometry of implant significantly affects the facet contact force (FCF). The FCF was maximum in C2, while C1 and C3 had similar values. It was assumed that the FCF increased due to the translation of vertebral body through the small curvature and decreased with large curvature because vertebral body rotates rather than translates.

The adjacent intervertebral disc stress was similar among surgical models. The disc stress was independent from geometry of implant.

Lastly, the implant stress tended to increase with increasing radius of curvature in extension, flexion and bending.

From these results, it turned out that the translation or rotation of the artificial disc depends on the curvature of ball-and-socket geometry. In the case with smaller curvature, the artificial disc translates through the curvature rather than rotates. Therefore, the facet contact force increases and the stress on implant also increases. Accordingly, the facet arthrosis at surgical level and subsidence of implant can be occurred. In addition, excessive motion could be generated in axial torsion.

On the other hand, in the case with larger curvature, the artificial disc rotates through the curvature rather than translates. Therefore, the facet contact force decreases and stress on implant also decreases compared to the values with small curvature. However, excessive motion can be occurred in all motion.

Therefore, the curvature of implant should be carefully considered to prevent undesired complications in the future clinical application.

In this study, the follower load which represents the intersegmental muscle force was not applied to the FE model. Therefore, physiologic condition

containing partial body weight and muscle force should be included in future study.

5 CONCLUSIONS

In this study, we investigated that the geometry of ball-and-socket implant can cause significant biomechanical changes including ROM, facet contact force at the surgical level. In addition, the geometry of implant affects the stress on implant itself. It is anticipated that this study can increase the understanding of different biomechanical effects with different curvature of implant at surgical level, and contribute to designing improved ball-and-socket artificial disc.

ACKNOWLEDGEMENTS

This work was supported by the grant from the institute of Medical System Engineering (iMSE) at GIST.

REFERENCES

- Bertagnoli, R., Yue, J. J., Nanieva, R., Fenk-Mayer, A., Husted, D. S., Shah, R. V., Emerson, J. W., 2006. *J. Neurosurg. Spine* 4, 85–90.
- Chen, S.-H., Zhong, Z.-C., Chen, C.-S., Chen, W.-J., Hung, C., 2009. *Med. Eng. Phys.* 31, 244–253.
- Godest, A. C., Beaugonin, M., Haug, E., Taylor, M., Gregson, P. J., 2002. *J. Biomech.* 35, 267–275.
- Kim, K.-T., Lee, S.-H., Suk, K.-S., Lee, J.-H., Jeong, B.-O., 2010. *J. Korean Neurosurg. Soc.* 47, 446–453.
- Mayer, M. H., Korge, A., 2002. *Eur. Spine J.* 11, S85–S91.
- Panjabi, M., Henderson, G., Abjornson, C., Yue, J., 2007. *Spine* 32, 1311–1319.
- Rohlmann, A., Zander, T., Bergmann, G., 2005. *Spine* 30, 738–743.
- Rundell, S. A., Auerbach, J. D., Balderston, R. A., Kurtz, S. M., 2008. *Spine* 33, 2510–2517.
- Yamamoto, I., Panjabi, M.M., Crisco, T., Oxland, T., 1989. *Spine* 14, 1256–1260.